Ferrer Ribera, RB.; Rogez, G.; Credi, A.; Ballardini, R.; Gandolfi, MT.; Balzani, V.; Liu, Y.... (2006). Photoinduced electron flow in a self-assembling supramolecular extension cable. Proceedings of the National Academy of Sciences. 103(49):18411-18416. doi:10.1073/pnas.060645910.

Photoinduced electron flow in a self-assembling supramolecular extension cable

1. Belén Ferrer * , † ,
2. Guillaume Rogez * , ‡ ,
3. Alberto Credi *,
4. Roberto Ballardini § , ¶ ,
5. Maria Teresa Gandolfi *,
6. Vincenzo Balzani * , ¶ ,
7. Yi Liu ⊥ , **,
8. Hsian-Rong Tseng ⊥ , †† , and
9. J. Fraser Stoddart ¶ , ⊥

Abstract

We report the design, bottom-up construction, characterization, and operation of a supramolecular system capable of mimicking the function played by a macroscopic electrical extension cable. The system is made up of a light-powered electron source, an electron drain, and a cable as the molecular components programmed to self-assemble by means of two distinct plug/socket junctions. Such connections are reversible and can be operated independently by orthogonal chemical inputs. In the source–connector–drain supermolecule, photoinduced electron transfer from source to drain occurs, and it can be switched off by dual-mode chemically controlled disassembling of the molecular components.

- electron transfer
- luminescence
- molecular device
- photochemistry
- supramolecular chemistry

Information processing at the molecular level could open the way to the design and construction of “molecular computers” (1) much smaller and more powerful than the current silicon-based computers. It can be noted that the term *molecular computer* is still an emotive one, despite the fact that more than 20 years ago the Pimentel report (2) was quite encouraging in this regard: There are those who dismiss as far-fetched the idea of man-made molecular scale computers.… But since we know that molecular computers are routine accessories of all animals from ants to zebras, it would be prudent to change the question from *whether* there will be man-made counterparts to questions concerning *when* they will come into existence and *who* will be leading in their development. The *when* question will be answered on the basis of fundamental research in chemistry; the *who* question will depend on which countries commit the required resource and creativity to the search. As research toward signal processing at the molecular level advances, it becomes more and more evident that two quite different strategies can be exploited. One strategy relies on the use of molecules to create nanoscale electric circuits that would replace those used in the current microelectronic

solid-state technology (3–6). An alternative strategy, which receives inspiration from information transfer processes in living organisms, is based on chemical input and output signals that can be generated by chemical, photochemical, and electrochemical reactions and combined with light inputs (absorption) and outputs (fluorescence, transmission) (7–14). The two strategies are different, not only in a philosophical sense, but also from a chemical viewpoint: molecules that are used as the components of a nanoscale electrical circuit in the solid state must be irreversibly linked together, whereas signal exchange among molecules in solution takes place by self-assembling/controlled-disassembling processes (15–20).

We report herein the design, bottom-up construction, characterization, and operation of a nanometric self-assembling system capable of performing signal processing in solution. In such a "wet" system that mimics, at the molecular level, the function served in the macroscopic world by an electric source, an extension cable, and a drain, the electron flow is driven by light and it is switched on/off by two distinct, reversible assembling/disassembling processes that are governed by chemical inputs and operate in series. The present system represents a substantial improvement on a previously described one (21), which was based on two (of three) different molecular components and could not mimic a real extension cable.

A system capable of exploiting the role of a working extension cable (Fig. 1 *A*) must consist of three components, programmed to operate as an electron source, a connecting wire, and an electron drain. The three components must be designed so that one end of the wire can be plugged in/out of the source, and the drain can be plugged in/out of the other end of the wire. Furthermore, each plug in/out function has to be reversible, independent, controllable by an external input, and monitorable. Finally, when the three parts are connected, an electron flow from the source to the drain must occur. The system made of components **1** $^{2+}$, **2**-H^{+}, and **3** $^{2+}$, shown in Fig. 1 *B*, meets these requirements at the (supra)molecular level.

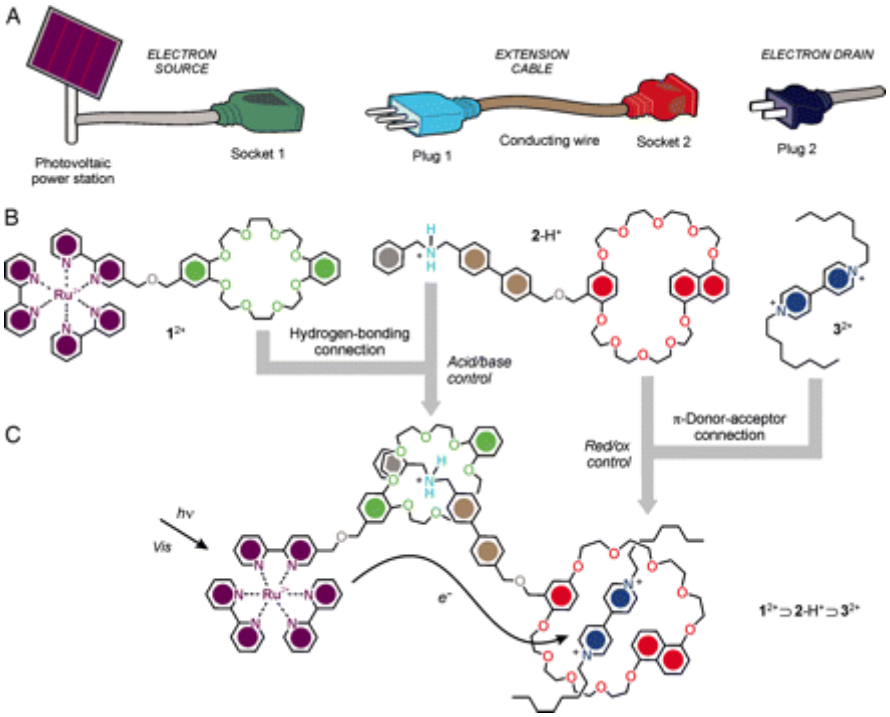

Fig. 1.

A chemical system capable of exploiting the role of a working extension cable. (*A*) In the macroscopic world, an electric extension cable is used to connect an electron source to an electron drain through a conducting wire and two different plug/socket devices that can be plugged in and out reversibly and independently from one another. The electron source is connected to a power station, e.g., a photovoltaic device. When the three parts are assembled, an electron flow from the source to the drain takes place. (*B* and *C*) The system made of components **1** $^{2+}$, **2**-H^{+}, and **3** $^{2+}$ in solution meets the above requirements at the (supra)molecular level. The electron source component **1** $^{2+}$ comprises a ruthenium-based visible-light-absorbing unit (violet), which is an electron donor in the excited state, and a dibenzo[24]crown-8 (DB24C8) unit (green) capable of playing the role of a hydrogen-bonding socket. The extension cable **2**-H^{+} is made up of a dialkylammonium ion center (cyan), which can thread as a plug into the DB24C8 socket, a conducting biphenyl spacer (maroon), and a benzonaphtho[36]crown-10 (BN36C10) unit (red), which plays the role of a π-electron-rich socket. The electron drain **3** $^{2+}$ contains a 4,4′-bipyridinium-type (viologen) unit (blue), which fulfills the role of a π-electron-acceptor plug for the BN36C10 socket; note that it cannot thread into the DB24C8 one. The three molecular species **1** $^{2+}$, **2**-H^{+}, and **3** $^{2+}$ self-assemble in solution to give the **1** $^{2+}$⊃**2**-H^{+}⊃**3** $^{2+}$ triad. In the fully connected **1** $^{2+}$⊃**2**-H^{+}⊃**3** $^{2+}$ system, excitation with visible light of the ruthenium-based photosensitizing unit of **1** $^{2+}$ is followed by electron transfer to **3** $^{2+}$, with **2**-H^{+} playing the role of an extension cable.

The electron source component **1** $^{2+}$ comprises (*i*) a $[Ru(bpy)_3]^{2+}$-type unit (bpy = 2,2′-bipyridine), which is an electron donor in its excited state (22), and (*ii*) a dibenzo[24]crown-8 (DB24C8) macrocycle capable of playing the role of a hydrogen-bonding socket (9, 21, 23). The extension cable **2**-H $^{+}$ is made up of three moieties, namely (*i*) a dialkylammonium ion center, which can insert itself as a plug into a DB24C8 socket, (*ii*) a conducting biphenyl spacer, and (*iii*) a benzonaphtho[36]crown-10 (BN36C10) unit, which fulfills the role of a π-electron-rich socket (9, 21). Finally, the 1,1′-dioctyl-4,4′-bipyridinium dication **3** $^{2+}$, which was selected among several bipyridinium derivatives because of its solubility in CH_2Cl_2, can play the role of an electron drain plug (9, 24). The two plug/socket connections **1** $^{2+}$⊃**2**-H^{+} and **2**-H^{+}⊃**3** $^{2+}$ can be controlled by acid/base and red/ox stimuli, respectively, and monitored by changes in the absorption and emission spectra. In the fully connected **1** $^{2+}$⊃**2**-H^{+}⊃**3** $^{2+}$ system, light excitation (25–27) of the ruthenium-based unit of **1** $^{2+}$ is followed by electron transfer to **3** $^{2+}$, with **2**-H^{+} playing the role of an extension cable (Fig. 1 *C*).

Compared with a previously described system (21), the one outlined in this article shows two conceptual and quite significant differences: (*i*) **2**-H^{+} consists of a plug and a socket components, and thus it really mimics an extension cable, whereas the previously used cable consisted of two plugs; (*ii*) the photoinduced electron transfer does take place from the first component, the ruthenium-based unit of **1** $^{2+}$, to the remote **3** $^{2+}$ viologen unit, whereas, in the previous system, the electron-receiving viologen unit was a component of the cable.

Results and Discussion

Properties of the Molecular Components.

Fig. 2 shows some of the compounds that have been used as references. Compound **1** $^{2+}$ exhibits, in the visible region, the absorption (λ_{max} = 450 nm, $\varepsilon = 1.4 \times 10^4$ liter·mol^{-1}·cm^{-1}) and emission (Figs. 3 *B* and 4; λ_{max} = 608 nm, τ = 333 ns) bands of its $[Ru(bpy)_3]^{2+}$ moiety, does not show redox processes in the range 0/−1 V versus the saturated calomel electrode (SCE), and is unaffected by addition of tributylamine (TBA) or zinc powder (see below). At $\lambda > 300$ nm, **2**-H$^+$ shows the same absorption spectrum as that of **2** (obtained by deprotonation of **2**-H$^+$ with one equivalent of TBA) and of the BN36C10 reference compound **4**. Each one of these three compounds exhibits the fluorescence band (Fig. 3 *A*; λ_{max} = 345 nm) of its 1,5-dimethoxynaphthalene unit. The emission intensity is the same in **2** and **4**, and much weaker (23%) in **2**-H$^+$ (see Fig. 6 and Table 1, which are published as supporting information on the PNAS web site). This behavior can be accounted for by a self-complexing conformation of **2**-H$^+$ (see *Supporting Text* and Fig. 7, which are published as supporting information on the PNAS web site), as that obtained when the two ends of a macroscopic extension cable are connected. The extended **2** and self-complexed **2**-H$^+$ forms can be interconverted reversibly by successive additions of trifluoromethanesulfonic acid (TFMS) and TBA; **2**-H$^+$ does not show any redox process in the range 0/−1 V versus SCE and does not react with zinc powder. Compound **3** $^{2+}$ exhibits an intense absorption band (λ_{max} = 258 nm), which is unaffected by addition of TFMS or TBA, and shows a reversible, one-electron reduction peak at −0.27 V versus SCE. Upon addition of zinc powder to deaerated solutions of **3** $^{2+}$, the dication is reduced to **3** $^+$, which shows the typical (24) absorption bands of a monoreduced viologen species.

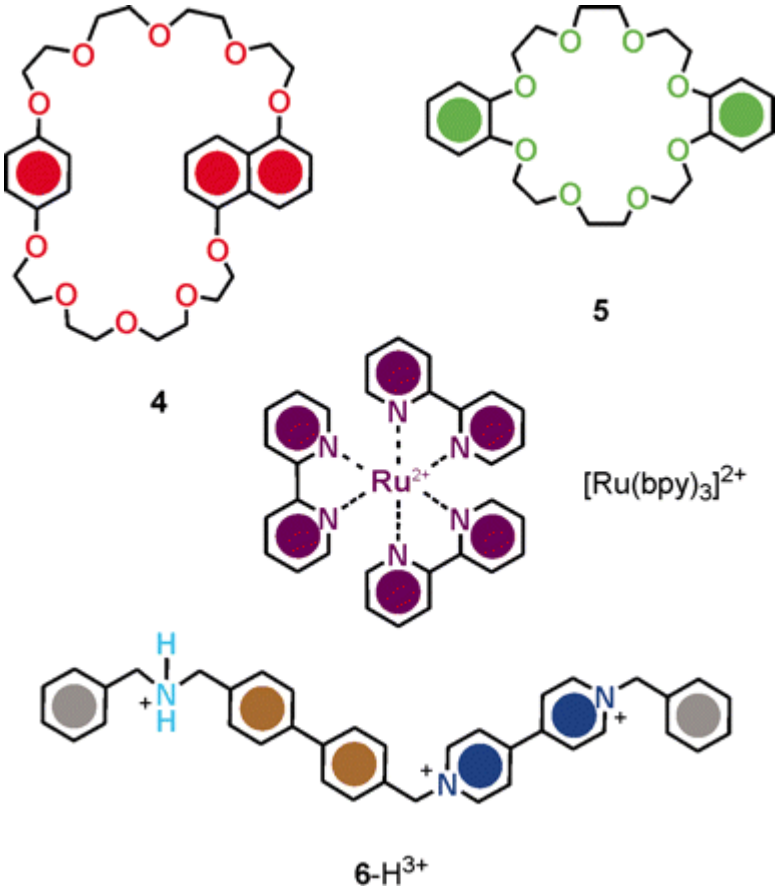

Fig. 2.

Reference compounds. $[Ru(bpy)_3]^{2+}$ and crown ethers BN36C10 (**4**) and DB24C8 (**5**) are models for the photosensitizing unit of **1** $^{2+}$ and for the socket units of **2**-H^+ and **1** $^{2+}$, respectively. The thread compound **6**-H^{3+} is used as a plug for the socket of **1** $^{2+}$ in competition experiments with **2**-H^+ (see text).

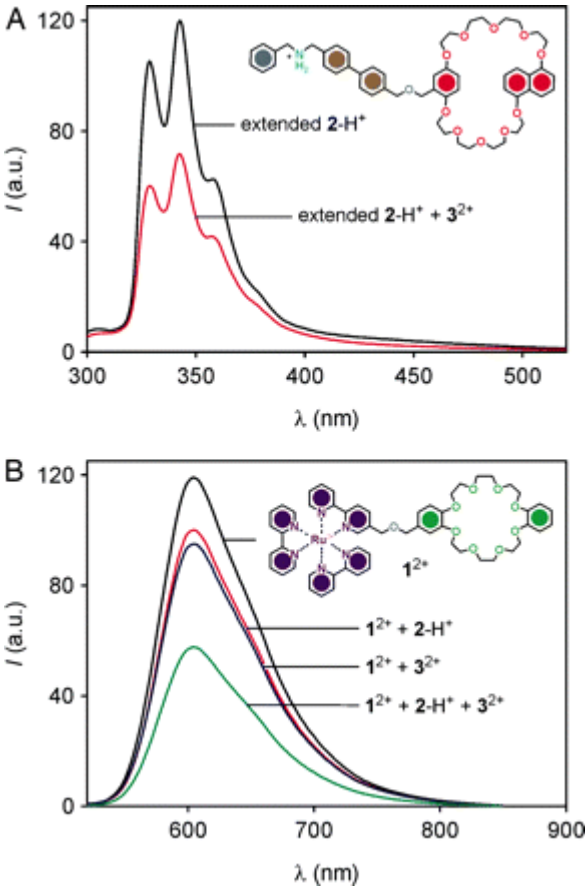

Fig. 3.

UV–visible emission measurements used to show the assembly of the molecular components. (*A*) Fluorescence spectra (λ_{exc} = 277 nm) of the BN36C10 moiety of **2**-H^+: black curve, extended **2**-H^+ (obtained by addition of crown ether 5 to self-threaded **2**-H^+, see text); red curve, extended **2**-H^+ + **3** $^{2+}$. a.u., arbitrary units. The emission intensity of a solution containing **1** $^{2+}$, **2**-H^+, and **3** $^{2+}$, after correction for inner filter effects caused by overlapping bands, coincides with that of the red curve within experimental errors. (*B*) Luminescence spectra (λ_{exc} = 450 nm) of the ruthenium-based unit of **1** $^{2+}$: black curve, **1** $^{2+}$ alone; red curve, **1** $^{2+}$ + **2**-H^+; blue curve, **1** $^{2+}$ + **3** $^{2+}$; green curve, **1** $^{2+}$ + **2**-H^+ + **3** $^{2+}$. Conditions: air-equilibrated CH_2Cl_2 solutions, room temperature; [**1** $^{2+}$] = 3.0×10^{-5} mol·liter^{-1}, [**2**-H^+] = 5.0×10^{-5} mol·liter^{-1}, and [**3** $^{2+}$] = 1.3×10^{-4} mol·liter^{-1}.

Self-Assembly and Controlled Disassembly of the Plug/Socket Supramolecular Dyads.

Titration of **2**-H^+ (2.0×10^{-5} mol·liter^{-1}) with the dibenzocrown ether **5** (Fig. 2) caused an increase in the fluorescence intensity of the BN36C10 moiety. It reaches a plateau after addition of 1 eq of **5** (see Fig. 8, which is published as supporting information on the PNAS web site), an observation which means that **5** opens up the self-complexed **2**-H^+ species, giving rise, as expected (23), to a stable ($K_a \approx 10^6$ liter·mol^{-1}) supramolecular entity **5**⊃**2**-H^+. Because **2**-H^+ pierces **5**, it should also penetrate the DB24C8 unit of **1** $^{2+}$. To evaluate the extent of association between **1** $^{2+}$ and **2**-H^+, we found the most convenient way was to perform a competition experiment with **6**-H^{3+} (Fig. 2), whose penetration of the DB24C8 unit of **1** $^{2+}$ ($K_a = 1 \times 10^5$ liter·mol^{-1}) can be

easily monitored (21). The results obtained showed that the **1** $^{2+}$⊃**2**-H^{+} hydrogen-bonding connection is robust ($K_a \approx 1 \times 10^6$ liter·mol^{-1}), reversible, and acid/base controllable.

Upon titration of **2**-H $^{+}$ with **3** $^{2+}$, no spectral change was observed. However, when the self-complexing conformation of **2**-H^{+} was opened up by addition of crown ether **5** (see above), titration with **3** $^{2+}$ caused a quenching of the BN36C10 fluorescence of **2**-H^{+} (Fig. 3 *A*; see also *Supporting Text* and Figs. 9–11, which are published as supporting information on the PNAS web site) and the appearance of a charge-transfer band (28) with λ_{max} = 487 nm, showing that the π-electron-donor macrocycle and the π-electron-acceptor wire associate (K_a = 7,400 liter·mol^{-1}). Addition of a 100-fold excess of zinc powder to a deaerated solution caused the appearance of the strong absorption band at 398 nm of the reduced **3** $^{+}$ unit (24) and a complete revival of the BN36C10 fluorescence, indicating that decomplexation had occurred. Therefore, the BN36C10 unit of **2**-H^{+} can play the role of a socket toward **3** $^{2+}$ when the dialkylammonium ion center is plugged in a DB24C8 unit and, under such conditions, the **2**-H $^{+}$ ⊃**3** $^{2+}$ connection can be red/ox controlled.

Self-Assembly of the Supramolecular Triad.

Next, we have examined the behavior of a solution containing all three components, **1** $^{2+}$, **2**-H^{+}, and **3** $^{2+}$ (Fig. 1). To measure corrected emission intensities and to disfavor bimolecular quenching processes, we used dilute solutions: [**1** $^{2+}$] = 3.0×10^{-5} mol·liter^{-1}, [**2**-H^{+}] = 5.0×10^{-5} mol·liter^{-1}, and [**3** $^{2+}$] = 1.3×10^{-4} mol·liter^{-1}. On the basis of the association constants mentioned above, under these conditions, >95% of **1** $^{2+}$ should be connected to **2**-H^{+} and ≈50% of the **1** $^{2+}$⊃**2**-H^{+} dyad should be connected with **3** $^{2+}$ to yield the **1** $^{2+}$⊃**2**-H $^{+}$ ⊃**3** $^{2+}$ triad. The real concentration of the triad was estimated by measuring the *static* quenching of the luminescence of the ruthenium-based unit of **1** $^{2+}$ by the **3** $^{2+}$ component, plugged into the BN36C10 moiety of **2**-H^{+}. Because **3** $^{2+}$ is also expected to quench the long-lived luminescence of the ruthenium-based unit of **1** $^{2+}$ by a dynamic process, we have first investigated the quenching of the luminescence of $[Ru(bpy)_3]^{2+}$ model compound and of the ruthenium-based unit of **1** $^{2+}$ by 1.3×10^{-4} mol·liter^{-1} **3** $^{2+}$ (in the absence of **2**-H^{+}), and found that, for both compounds, quenching of emission intensity (Fig. 3 *B*) and lifetime (Fig. 4) take place. In particular, the lifetime of the ruthenium-based unit of **1** $^{2+}$ decreased from 333 to 266 ns. Then we measured the quenching of the luminescence intensity (taken as 100) and lifetime (336 ns) of the **1** $^{2+}$⊃**2**-H^{+} dyad upon addition of 1.3×10^{-4} mol·liter^{-1} **3** $^{2+}$. We found that the emission intensity was reduced to 58 (Fig. 3 *B*) and that a triple-exponential decay took place, corresponding to lifetimes of 260, 75, and 7 ns (Fig. 4 and Table 2, which is published as supporting information on the PNAS web site). The longest lifetime can be attributed straightforwardly to the dynamic quenching process, which, from quantitative analysis, accounts for 27% of the observed quenching—in reasonable agreement with the 20% of quenching found in the absence of **2**-H^{+}. The two shorter lifetimes, accounting for the remaining 15% of quenching, can be assigned to static quenching processes taking place in two different (co)-conformations, possibly stretched and folded, of the **1** $^{2+}$⊃**2**-H $^{+}$ ⊃**3** $^{2+}$ triad.

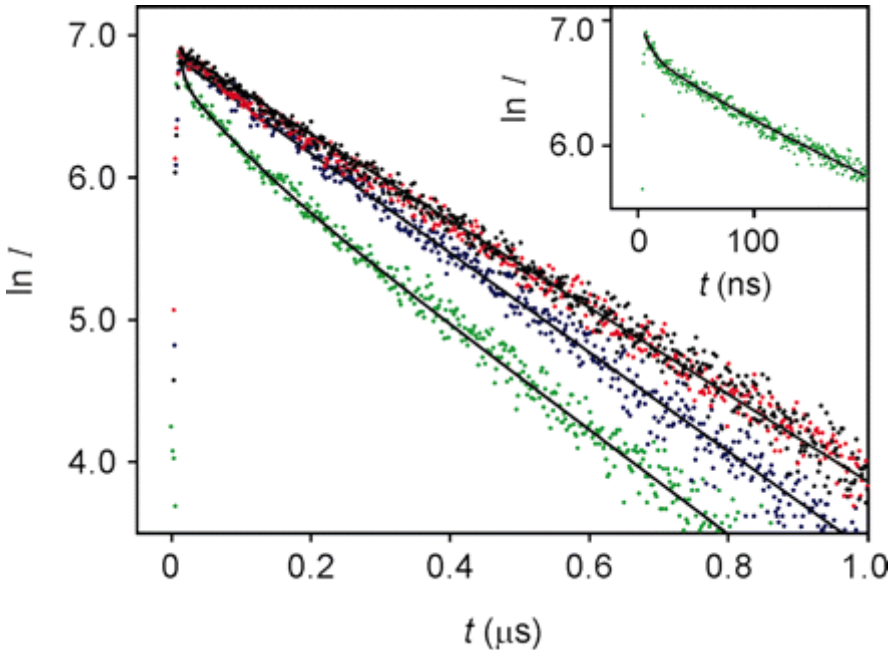

Fig. 4.

Decay of the ruthenium-based luminescence (λ_{exc} = 407 nm) for **1** $^{2+}$ alone (black dots) and in the presence of **2**-H^{+} (red), **3** $^{2+}$ (blue), and **2**-H^{+} + **3** $^{2+}$ (three-component system, green). *I*, intensity of luminescence. The first three data sets correspond to single-exponential decays, whereas the latter (see *Inset* for a detail) corresponds to a triple-exponential decay. The fitted curves are represented as full lines. The experimental conditions are the same as those described for Fig. 3.

Photoinduced Electron Flow in the Supramolecular Triad.

Direct observation of the visible-light-induced electron flow from the ruthenium-based unit of **1** $^{2+}$ to **3** $^{2+}$ in the fully connected triad came from transient absorption experiments. Selective excitation of the ruthenium-based unit of **1** $^{2+}$ with nanosecond laser pulses (532 nm) in deaerated solutions containing the three components led to the prompt (within the laser pulse) appearance of an absorption signal at 398 nm (Fig. 5), where the monoreduced **3** $^{+}$ species exhibits (24) an intense absorption band. Such a signal, which was not present in the control solution, decays according to a first-order process with a lifetime of 28 ns.

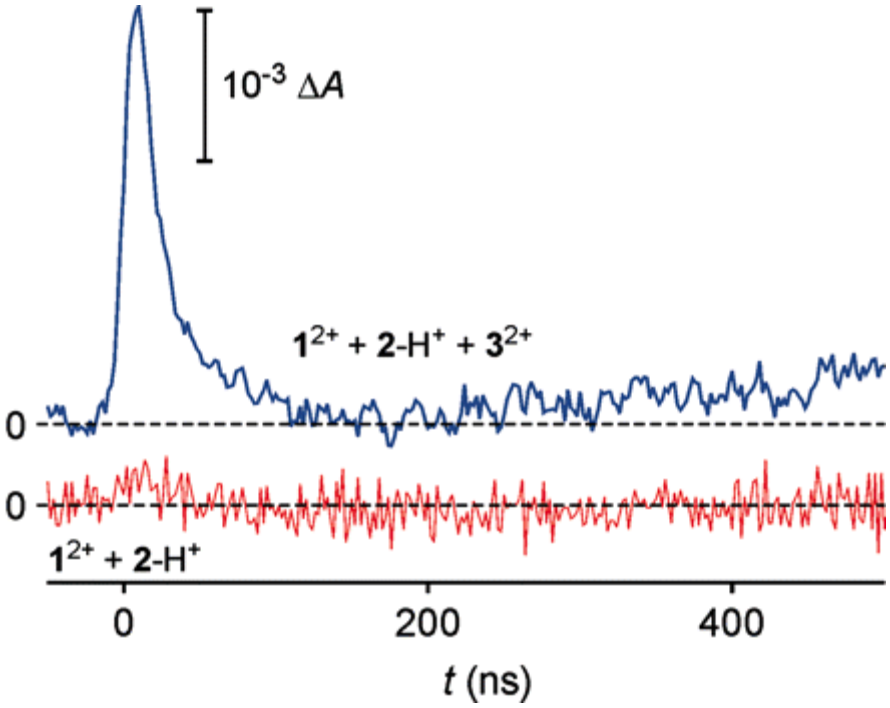

Fig. 5.

Transient absorption kinetics monitored at 398 nm (isosbestic point between the ground and excited ruthenium-based unit) upon nanosecond laser excitation at 532 nm of solutions containing **1** $^{2+}$, **2**-H^{+}, and **3** $^{2+}$ (blue), and only **1** $^{2+}$ and **2**-H^{+} as a control (red). The immediate increase and the successive fast decrease (τ = 28 ns) of absorbance is assigned to the formation and disappearance of the **3**$^{+}$ species in the **1** $^{2+}$⊃**2**-H^{+}⊃**3** $^{2+}$ triads, and the signal after 200 ns is assigned to the **3**$^{+}$ species originating from the dynamic quenching of the ruthenium-based unit of **1** $^{2+}$ by **3** $^{2+}$. Conditions: deaerated CH_2Cl_2 solutions, room temperature; [**1** $^{2+}$] = 3.7×10^{-5} mol·liter^{-1}, [**2**-H^{+}] = 4.6×10^{-5} mol·liter^{-1}, and [**3** $^{2+}$] = 3.0×10^{-5} mol·liter^{-1}.

The concentration of the **1** $^{2+}$⊃**2**-H^{+}⊃**3** $^{2+}$ species in the solution containing all three components was also estimated by measuring the quenching of the BN36C10 fluorescence by the **3** $^{2+}$ component plugged into the BN36C10 moiety of **2**-H^{+} (Fig. 3 *A*). In this case, dynamic quenching processes do not interfere because of the short lifetime (7 ns) of the BN36C10 excited state. The results obtained from intensity quenching are comparable to those obtained for the quenching of the ruthenium-based unit of **1** $^{2+}$. They are, however, somewhat less precise because of interference caused by band overlapping. The quenched lifetimes were too short to be measured, in keeping with similar systems (21).

Controlled Disassembly of the Extension Cable System.

Addition of one equivalent of TBA to the solution containing the three components caused an 11% increase in the luminescence intensity of the ruthenium-based unit of **1** $^{2+}$, in agreement, within experimental errors, with the 15% quenching attributed to the presence of **1** $^{2+}$⊃**2**-H^{+}⊃**3** $^{2+}$ triad (see above). Moreover, a monoexponential luminescence decay was restored. These results show that the **1** $^{2+}$⊃**2**-H $^{+}$ junction of the triad can be acid/base controlled. Addition of a 20-fold excess of zinc powder to deaerated solutions containing the three components caused, besides the appearance of

the strong absorption bands for **3** $^{+}$ (see Fig. 12, which is published as supporting information on the PNAS web site), a revival of the BN36C10 fluorescence of the **2**-H^{+} unit, showing that the **2**-H $^{+}$ ⊃**3** $^{2+}$ connection can be red/ox controlled.

Conclusion

We have designed, synthesized, and characterized a multicomponent molecular level system that operates in CH_2Cl_2 solution and mimics the function played in the macroscopic world by a light-powered electric source, an extension cable, and a drain (Fig. 1). In the self-assembled, fully connected **1** $^{2+}$⊃**2**-H^{+}⊃**3** $^{2+}$ supramolecular system, electrons generated by visible photoexcitation of the ruthenium-based unit of **1** $^{2+}$ are transmitted to **3** $^{2+}$ on the nanosecond time scale. The system can be switched on/off by two distinct, reversible assembling/disassembling processes that are governed by chemical inputs operating in series and therefore can play the role of an NAND logic gate.

The present system represents a substantial improvement on a previously described one (21) that was based on different molecular components. In particular, **2**-H $^{+}$ consists of a plug and a socket components and thus it really mimics an extension cable. Furthermore, at variance with the previously reported system (21), the photoinduced electron transfer does take place from the first component, the ruthenium-based unit of **1** $^{2+}$, to the remote **3** $^{2+}$ viologen unit. It may be noticed that, in the present supramolecular system, electrons do not flow through the intermediate component in the same way as they do in the metallic wire of a macroscopic extension cord. Nevertheless, the electron transfer in the system discussed in this article takes place most likely by a superexchange mechanism that implies an electronic role of the bridge.

Interestingly, the extension cable component **2**-H^{+} exists in a self-threaded conformation, which cannot host the electron drain until it is opened up by complexation with the socket unit of the source component. This feature, which can be viewed as a limitation because it reduces the efficiency, in fact plays the function of a safety-catch device. Moreover, the photoinduced electron-transfer process can be powered by sunlight because the $[Ru(bpy)_3]^{2+}$-type component shows a broad and intense absorption band in the visible spectral region.

Materials and Methods

The synthesis and characterization of **1** $^{2+}$ and **6**-H^{3+} have been reported elsewhere (21). 1,1′-Dioctyl-4,4′-bipyridinium **3** $^{2+}$, crown ether **4**, and $[Ru(bpy)_3][PF_6]_2$ were available from previous investigations. Crown ether **5** (Aldrich, Milwaukee, WI), TBA (Fluka, Buchs, Switzerland), trifluoromethanesulfonic acid (Fluka), and the solvent CH_2Cl_2 used for the photophysical (Uvasol from Merck, Darmstadt, Germany) and electrochemical (Hi-Dry from ROMIL, Cambridge, U.K.) experiments were used as received. The synthesis of compound **2**-H^{+} is outlined in Scheme 1, which is published as supporting information on the PNAS web site. More details can be found in the *Supporting Text*.

The absorption and luminescence experiments have been performed at room temperature (≈300 K) on dilute solutions (2.0×10^{-5} to 2.0×10^{-4} mol·liter^{-1}) in air-

equilibrated CH_2Cl_2 (Merck Uvasol), unless otherwise stated. UV–visible absorption spectra were recorded with a λ40 spectrophotometer (Perkin-Elmer, Wellesley, MA). Luminescence spectra were obtained with a LS-50 spectrofluorimeter (Perkin-Elmer) equipped with a R928 phototube (Hamamatsu, Hamamatsu City, Japan). Luminescence lifetimes were measured by the time-correlated single-photon counting (TCSPC) technique with Edinburgh Instruments (Livingston, U.K.) TCSPC equipment. The exciting light was produced by a gas arc lamp (model nF900, filled with D_2) or a laser diode (λ_{exc} = 407 nm) that delivered pulses of ≈1 ns (full width at mid-height). The light emitted was filtered by using a cutoff filter, and the detector was a cooled Hamamatsu R928 photomultiplier. More details on the fitting of the experimental luminescence decay curves and on the absorption and luminescence titration experiments can be found in the *Supporting Text*. The experimental error on molar absorption coefficients, emission intensities, and luminescence lifetimes is estimated to be ±5%. The error on the association constants, derived from titration experiment, is estimated to be ±20%.

Transient absorption experiments were performed at room temperature by exciting the sample with 10-ns (full width at mid-height) pulses of a Surelite I-10 Nd:YAG laser (Continuum, Santa Clara, CA). A 150-W xenon lamp (model 720; power supply, model 620; Applied Photophysics, Surrey, U.K.) perpendicular to the laser beam was used as a probing light; for the kinetic investigations in the 0– to 10-μs time window, a pulsing unit (Applied Photophysics model 03–102, 2-ms pulses) was also used. Excitation was performed at λ = 532 nm (obtained by frequency doubling). A shutter was placed between the lamp and the sample, and it was opened only during the measurements to prevent phototube fatigue and photodecomposition. Suitable pre- and post-cutoff and bandpass filters were also used to avoid photodecomposition and interferences from scattered light. The light was collected in a PTI (South Brunswick, NJ) monochromator (model 01-001; grating, 1,200 lines per mm; slit width, 0.25 mm; resolution, 1 nm), detected by a Hamamatsu R928 tube, and recorded on a Tektronix (Vimodrone, Italy) TDS380 (400 MHz) digital oscilloscope connected to a PC. Synchronous timing of the system was achieved by means of a built-in-house digital logic circuit. The absorption transient decays were plotted as $\Delta A = \log(I_0/I_t)$ versus time, where I_0 and I_t are the probing light intensity before the laser pulse and after delay t, respectively. Each decay was obtained by averaging at least 20 pulses. Transient absorption spectra were obtained from the decays measured at various wavelengths (10-nm increment), by sampling the absorbance changes at constant delay time. The experimental error on the wavelength and lifetime values is estimated to be ±2 nm and ±5%, respectively.

Voltammetric measurements (cyclic voltammograms, CVs, and differential pulse voltammograms, DPVs) were recorded in argon-purged CH_2Cl_2 (ROMIL Hi-Dry) solution at room temperature with an Autolab 30 multipurpose instrument (Eco Chemie, Origgio, Italy) interfaced to a PC. The concentration of the compounds examined was 5.0×10^{-4} mol·liter^{-1}; 0.050 mol·liter^{-1} tetraethylammonium hexafluorophosphate was added as the supporting electrolyte. The working electrode was a glassy carbon microelectrode (0.08 cm^2). A complete description of the electrochemical cell and the electrochemical procedures is reported in the *Supporting Text*. The accuracy on the potential values is estimated to be ±10 mV.

Acknowledgments

This research was supported by the Ministry of Education, University and Research in Italy (Programmi di Ricerca di Interesse Nazionale “Supramolecular Devices” and the Fondo per gli Investimenti della Ricerca di Base RBNE019H9K), and by the National Science Foundation (CHE0317170) in the United States. We acknowledge the European Union for support under the auspices of the Molecular-Level Devices and Machines Network (HPRN-CT-2000-00029), the Biomach Specific Targeted Research Project (NMP2-CT-2003-505487), and a Marie Curie Individual Fellowship to B.F. (HPMF-CT-2002-01916).

Footnotes

- [¶]To whom correspondence may be addressed. E-mail: vincenzo.balzani@unibo.it, rballard@ciam.unibo.it, or stoddart@chem.ucla.edu
- Author contributions: A.C., R.B., M.T.G., V.B., and J.F.S. designed research; B.F., G.R., Y.L., and H.-R.T. performed research; G.R., R.B., and M.T.G. analyzed data; and A.C., V.B., and J.F.S. wrote the paper.
- [†]Present address: Departamento de Química, Universidad Politécnica de Valencia, Camino de Vera s/n, 46022 Valencia, Spain.
- [‡]Present address: Institut de Physique et de Chimie des Materiaux de Strasbourg, Unité Mixte de Recherche 7504, 23 rue du Loess, B.P. 43, 67034 Strasbourg Cedex 2, France.
- **Present address: Department of Chemistry and The Skaggs Institute for Chemical Biology, The Scripps Research Institute, 10550 North Torrey Pines Road, La Jolla, CA 92037.
- [††]Present address: Department of Molecular and Medical Pharmacology and The Crump Institute for Molecular Imaging, University of California, Los Angeles, CA 90095.
- The authors declare no conflict of interest.
- This article is a PNAS direct submission.
- Abbreviations:

  bpy,
  2,2′-bipyridine;
  BN36C10,
  benzonaphtho[36]crown-10;
  DB24C8,
  dibenzo[24]crown-8;
  SCE,
  saturated calomel electrode;
  TBA,
  tributylamine.

References

1. Ball P (2000) Nature 406:118–120.

2. Board on Chemical Sciences and Technology (1985) Opportunities in Chemistry

(Natl Acad Press, Washington, DC).

3. Joachim C, Gimzewski JK, Aviram A (2000) Nature 408:541–548.

4. Metzger RM (2003) Chem Rev 103:3803–3834.

5. Flood AH, Stoddart JF, Steuerman DW, Heath JR (2004) Science 306:2055–2056.

6. Blum AS, Kushmerick JG, Long DP, Patterson CH, Yang JC, Henderson JC, Yao Y, Tour JM, Shashidhar R, Ratna BR (2005) Nature Mat 4:167–172.

7. Balzani V, Credi A, Venturi M (2003) Molecular Devices and Machines: A Journey into the Nano World (Wiley-VCH, Weinheim, Germany).

8. Kelly TR, ed (2005) Molecular Machines, Topics in Current Chemistry (Springer, New York), Vol 262.

9. Balzani V, Credi A, Raymo FM, Stoddart JF (2000) Angew Chem Int Ed 39:3348–3391.

10. de Silva AP, McClenaghan ND (2004) Chem Eur J 10:574–586.

11. de Silva AP (2005) Nature Mat 4:15–16.

12. Margulies D, Melman G, Shanzer A (2006) J Am Chem Soc 128:4865–4871.

13. Langford SJ, Yann T (2003) J Am Chem Soc 125:11198–11199.

14. Raymo FM (2002) Adv Mater 14:401–414.

15. Philp D, Stoddart JF (1996) Angew Chem Int Ed Engl 35:1155–1196.

16. Lehn J-M (2002) Science 295:2400–2403.

17. Balzani V, Credi A, Venturi M (2002) Proc Natl Acad Sci USA 99:4814–4817.

18. Cooke G, Rotello VM (2002) Chem Soc Rev 31:275–286.

19. Kaifer AE (1999) Acc Chem Res 32:62–71.

20. Amendola V, Fabbrizzi L, Pallavicini P (2001) Coord Chem Rev 216–217:

435–448.

21. Ballardini R, Balzani V, Clemente-Leo´n M, Credi A, Gandolfi MT, Ishow E,

Perkins J, Stoddart JF, Tseng H-R, Wenger S (2002) J Am Chem Soc

124:12786–12795.

22. Juris A, BalzaniV, Barigelletti F, Campagna S, Belser P, von ZelewskyA(1988)

Coord Chem Rev 84:85–277.

23. Ashton PR, Ballardini R, Balzani V, Go´mez-Lo´pez M, Martı´nez-Dı´az M-V,

Montalti M, Piersanti A, Prodi L, Stoddart JF, Williams DJ (1997) J Am Chem

Soc 119:10641–10651.

24. Monk PMS (1998) The Viologens: Physicochemical Properties, Synthesis and

Application of the Salts of 4,4————————————-Bipyridine (Wiley, Chichester, UK).

25. Gust D, Moore TA, Moore AL, Lee S-J, Bittersmann E, Luttrull DK, Rehms

AA, DeGraziano JM, Ma XC, Gao F, et al. (1990) Science 248:199–201.

26. Wasielewski MR (1992) Chem Rev 92:435–461.

27. Piotrowiak P (1999) Chem Soc Rev 28:143–150.

28. Ashton PR, Ballardini R, Balzani V, Credi A, Gandolfi MT, Menzer S,

Pe´rez-Garcı´a L, Prodi L, Stoddart JF, Venturi M, et al. (1994) J Am Chem Soc

117:11171–11197.